Self-sustained Inertial Oscillations*

JOSEPH PEDLOSKY AND HENRY STOMMEL†

Department of Physical Oceanography, Woods Hole Oceanographic Institution, Woods Hole, Massachusetts

(Manuscript received 24 February 1992, in final form 2 November 1992)

ABSTRACT

The authors describe a self-sustaining baroclinic inertial oscillation whose energy source rests in a uniform horizontal temperature gradient. This energy is released through the agency of a stratification-dependent mixing law that is meant to crudely model the occurrence of enhanced mixing when the stratification weakens. The mixing is chosen to be negligible over most of the cycle and large only when the stratification is small.

Sustained inertial oscillations are shown to be the natural end state of the instability of possible steady solutions when the decrease of the mixing rate with temperature exceeds a critical value. If the variation of the mixing rate with temperature is abrupt, a finite-amplitude oscillation is sustained, although a possible steady solution is linearly stable.

1. Introduction

In the course of some numerical experiments carried out by one of us on a model of an oceanic surface layer with a horizontal density gradient, it was noticed that self-excited inertial oscillations could occur. Qualitatively, the oscillation can be related to the model's parameterization of mixing in the following way. In the numerical model, which has many layers in the vertical, the layers respond to the presence of an imposed baroclinic pressure gradient with a geostrophic adjustment process. Although the whole layer is initially supposed to be vertically well mixed, the subsequent adjustment in the presence of the horizontal temperature gradient increases the stratification. During adjustment, the accompanying inertial oscillation causes an overshoot of the possible geostrophically balanced state, and the stratification becomes so weak that vertical mixing is enhanced, quenching the motion. The system thus finds itself again in an unbalanced state and proceeds to restart the adjustment process reactivating the inertial oscillation. The cycle was observed to repeat indefinitely.

Our purpose in this paper is to examine a very simple model of a self-sustained inertial oscillation with a qualitative similarity to the more complicated model of the original numerical experiment. Our method is to construct a system with as few working parts as possible, which yet reproduces the phenomenon of self-excited oscillations. The central mechanism of our model is a simple stratification-dependent mixing law. We show below that if the mixing increases with decreasing stratification, self-sustained oscillations can result spontaneously.

In section 2, we describe the physical model and discuss the possible steady states. An energy argument is described that demonstrates that sustained oscillations about this steady solution are possible with a mixing coefficient that decreases with increasing stratification. In section 3, we discuss the instability of the steady solution that results when a "soft" mixing law is used, that is, one in which the dissipation smoothly decreases with stratification. Although less relevant than the "hard" mixing law of the subsequent section (for which the dissipation is an abrupt function of temperature), the "soft" law has important advantages of analytical tractability and usefully demonstrates the instability of the steady solution. Section 4 describes the "hard" mixing scenario in which the mixing suddenly increases when a minimum stratification threshold is passed. Numerical and analytical evidence is presented for the existence of persistent self-excited oscillations.

In all cases, the ultimate energy source for the motion rests in the imposed baroclinic pressure gradient, which, in turn, is a consequence of a large-scale temperature gradient in the surface layer. It is the temperature de-

* Woods Hole Oceanographic Institution Contribution No. 7999.

† *Note:* Henry Stommel and I concluded this work and discussed how we would present it before he entered the hospital in January 1992. However, he died before ever seeing the manuscript. Thus, although it represents joint work and many of the ideas, as usual, were Hank's, I take full responsibility for errors of analysis or interpretations herein.—J.P.

Corresponding author address: Dr. Joseph Pedlosky, Department of Physical Oceanography, Woods Hole Oceanographic Institution, Woods Hole, MA 02543.

pendence of the mixing that allows this steady forcing to become tapped for the sustained inertial oscillations.

2. The model

Our goal is to provide the simplest model to describe the generation of inertial oscillations seen in the previously noted numerical experiments. The heart of the mechanism is the quenching of the baroclinic velocity by vertical mixing for weak or unstable stratification. It seemed to us then that a two-layer model was the maximum permissible simplification containing that process. Therefore, consider a model of the oceanic surface layer partitioned into two layers of equal depth h (see Fig. 1) in which there is a preexisting large-scale horizontal temperature variation. Each layer then has initially the same temperature, and the two-layer model is the minimum resolution of the baroclinic structure that subsequently develops. We take the large-scale temperature gradient, in the x direction, to be constant; for example,

$$\frac{\partial T}{\partial x} = -B, \tag{2.1}$$

from which, with the hydrostatic approximation,

$$\frac{\partial p}{\partial x} = -\rho_0 \alpha g B z, \tag{2.2}$$

where α is the coefficient of thermal expansion and ρ_0 is the mean density, and where z is measured from the interface between the two layers. In deriving (2.2) from (2.1), we have assumed that there is no vertically averaged pressure gradient; that is, we are concentrating on the baroclinic response of the fluid. To simplify matters further, we also assume that the velocities in each layer are z independent and respond to the vertically averaged pressure gradient. In the upper layer this yields

$$\left\langle \frac{\partial p}{\partial x} \right\rangle = -\rho_0 \alpha g B \frac{h}{2},$$

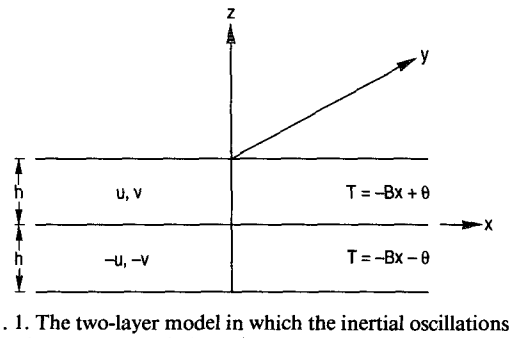

FIG. 1. The two-layer model in which the inertial oscillations take place. A large-scale, spatially variable temperature field, $T = -Bx$, exists in both layers. The subsequent baroclinic pressure gradient drives a purely baroclinic velocity field (u, v) and $(-u, -v)$ in each layer. The temperature perturbation is produced by the motion in θ $(-\theta)$ in the upper (lower) layer. These fields are spatially constant.

while in the lower layer the pressure gradient is equal but of opposite sign. The application of this horizontally uniform pressure gradient will give rise to velocities (u, v) and temperature anomaly θ in the upper layer that are also horizontally uniform in space and equal and opposite to those produced in the lower layer. We further suppose that momentum and temperature are dissipated by simple Rayleigh friction and Newtonian cooling proportional to the velocity differences between the two layers. Although the coefficients of friction and cooling could be distinct, indeed there is a conceptual advantage in keeping track of which dissipation mechanism is important; for mathematical simplicity we take them to be equal.

Under these simplifications the velocity and temperature anomalies satisfy

$$\frac{du}{dt} - fv = \rho_0 \alpha g B \frac{h}{2} - Au,$$

$$\frac{dv}{dt} + fu = -Av,$$

$$\frac{d\theta}{dt} - uB = -A\theta, \tag{2.3a,b,c}$$

where f is the Coriolis parameter and A is the mixing coefficient. Note that the vertical stratification of the two-layer model is proportional to θ.

It is convenient to introduce as scales for time, velocity, and temperature, f^{-1}, $\rho_0 \alpha g B h/2f$, and $\rho_0 \alpha g B^2 h/2f^2$, respectively. In terms of these scales, the nondimensional equations of motion are

$$\frac{du}{dt} - v = 1 - au,$$

$$\frac{dv}{dt} + u = -av,$$

$$\frac{d\theta}{dt} - u = -a\theta. \tag{2.4a,b,c}$$

Our interest is in the case where the mixing coefficient a is a function of the stratification θ. In all cases, we expect the mixing to decrease if the stratification is enhanced. We consider two "laws" of mixing. The first is the "soft" or smooth law

$$a = a_m e^{-m_1 \theta}, \tag{2.5}$$

in which $a(\theta)$ decreases smoothly as the stratification increases. The second case is the "hard" or abrupt law

$$a = \begin{cases} a_h, & \theta > \theta_c, \\ a_c, & \theta < \theta_c, \end{cases} \tag{2.6}$$

where $a_c \gg a_h$, so that the mixing parameter suddenly increases when θ falls below the critical value θ_c. In place of (2.6), its analytical equivalent will on occasion be used,

$$a = \frac{1}{2}\{(a_h + a_c) + (a_h - a_c)\tanh m_2(\theta - \theta_c)\}, \tag{2.7}$$

where m_2 is large. This latter form is convenient for numerical calculation.

Steady solutions of (2.4a,b,c) can be found as

$$v_0 = -\frac{1}{1 + a_0^2} = -\theta_0,$$

$$u_0 = \frac{a_0}{1 + a_0^2}, \tag{2.8a,b}$$

where

$$a_0 \equiv a(\theta_0). \tag{2.9}$$

If a were constant, or if $a(\theta)$ satisfies the "soft" law, a little thought shows that only a single simultaneous solution of (2.8a) and (2.5) is possible. If $a(\theta)$ is given by (2.7), however, three steady solutions are possible as demonstrated in Fig. 2. If a_c or θ_c are too small, only one steady solution exists as indicated by the intersection of the curves in the figure. If the discontinuous "hard" law (2.6) is used, the third, intermediate, solution is undefined, that is, nonexistent.

Our interest lies in both the linear stability of the steady solutions and the dynamics of finite-amplitude sustained oscillations, that is, the possibility of limit cycles.

In the latter case, it is helpful to introduce v_a as the departure of v from its geostrophic value; that is,

$$v = -1 + v_a, \tag{2.10}$$

since the inertial oscillations to be described are oscillations about the geostrophic value. Thus, the complete ageostrophic velocity (u, v_a) satisfies

$$\frac{du}{dt} - v_a = -au,$$

$$\frac{dv_a}{dt} + u = -a(v_a - 1). \tag{2.11a,b}$$

An energy equation for the ageostrophic motion may be found as

$$\frac{d}{dt}\frac{(u^2 + v_a^2)}{2} = -a(v_a^2 + u^2) + av_a, \tag{2.12}$$

and we note that the sign of the final term in (2.12) is a priori indeterminant.

At the same time, following (2.8a),

$$\theta = 1 + \theta_a, \tag{2.13}$$

so that θ_a satisfies

$$\frac{d\theta_a}{dt} - u = -a(1 + \theta_a). \tag{2.14}$$

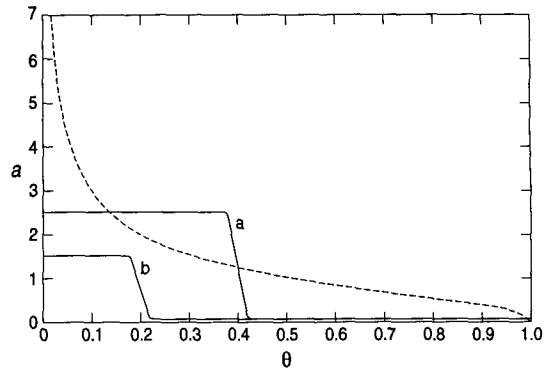

FIG. 2. The dashed curve represents the steady solution for θ versus the dissipation coefficient $a(\theta)$ (for the case $k = a$). Curves (a) and (b) represent two mixing laws. In each case, there is low (high) dissipation at high (low) stratification, θ. In case (a) there are three possible steady solutions. In case (b) there is only one.

Adding (2.11b) and (2.14) yields

$$\frac{d}{dt}(\theta_a + v_a) = -av_a - a\theta_a. \tag{2.15}$$

Now suppose we inquire as to whether a sustained oscillation of the ageostrophic velocity is possible. A numerical example demonstrating that such a limit cycle solution can exist is shown in Fig. 3 for the case where a is given by (2.7) with $a_h = 0.1$, $a_c = 0.15$, and $m_2 = 100$.

If (2.12) is averaged over a period of the oscillation, it follows that

$$\overline{a(v_a^2 + u^2)} = \overline{av_a}, \tag{2.16}$$

where an overbar denotes an average over a cycle of the oscillation. As shown in the figure, v_a has, very nearly, a zero average itself so that the equality (2.16) would be impossible if $a(\theta)$ were constant unless $v_a = u = 0$.

A similar average of (2.15) yields

$$\overline{av_a} = -\overline{a\theta_a}. \tag{2.17}$$

Since $a(\theta_a)$, we may use the mean value theorem to write

$$\overline{a\theta_a} = a(\theta_*)\overline{\theta_a} + \frac{\partial a}{\partial \theta}(\theta_*)\overline{\theta_a^2}, \tag{2.18}$$

where θ_* is a temperature within the range of the oscillation of the temperature over a cycle. If $\overline{\theta_a}$ (as $\overline{v_a}$) is essentially zero, it follows from (2.16), (2.17), and (2.18) that a necessary condition for the sustained oscillation to occur is that

$$\frac{\partial a}{\partial \theta}(\theta_*) < 0. \tag{2.19}$$

That is, for at least some part of the temperature (stratification) experienced by the fluid during the oscillation

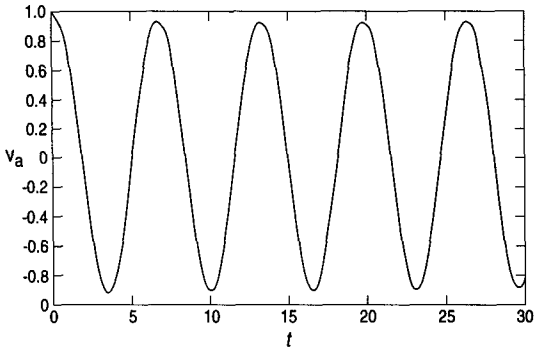

FIG. 3. The sustained inertial oscillation for the case $a_h = 0.01$, $a_c = 1.5$, $T_c = 0.15$, and $m_2 = 100$. Time is scaled with f^{-1}. The oscillation period is very nearly $2\pi/f$.

the mixing coefficient must decrease with increasing stratification. Otherwise, the oscillations will decay and the solution will inexorably converge to the steady solution (2.8). In the next sections we examine in detail the nature of the instability of the steady solutions and the resulting finite-amplitude oscillations.

3. "Soft" instability

In this section, we describe the instability of the steady solutions (2.8) when (2.5) applies. In all cases of interest, $a_0 = a(\theta_0)$ turns out to be small. This suggests that an analytical approach might be helpful in illuminating the basic instability that stimulates the self-sustained oscillation. This factor, plus the simple analytical representation of $a(\theta)$ provided by the special form of (2.5), provides the major motivation for selecting an otherwise artificial mixing rule.

To describe the stability of the steady solution, each variable is written as a sum of the steady solution, (2.6), plus a perturbation denoted by a prime; that is,

$$\begin{aligned} v &= v_0 + v', \\ u &= u_0 + u', \\ \theta &= \theta_0 + \theta'. \end{aligned} \tag{3.1}$$

The equations for the prime variables are

$$\begin{aligned} \frac{\partial u'}{\partial t} &= v'[a(u_0 + u') - a_0 u_0] - a_0 \frac{\partial u'}{\partial \tau}, \\ \frac{\partial v'}{\partial t} &= -u'[a(v_0 + v') - a_0 v_0] - a_0 \frac{\partial v'}{\partial \tau}, \\ \frac{\partial \theta'}{\partial t} &= u'[a(\theta_0 + \theta') - a_0 \theta_0] - a_0 \frac{\partial \theta'}{\partial \tau}, \end{aligned} \tag{3.2a,b,c}$$

where we have also introduced the slow development time

$$\tau = a_0 t$$

so that each variable is explicitly a function of t and τ. Thus, d/dt in (2.3) is transformed to $(\partial/\partial t) + [a_0(\partial/\partial \tau)]$.

The perturbations are now expanded in an asymptotic series in a_0; that is,

$$v' = v_1 + a_0 v_2 + \cdots,$$

which when used in (3.2) yields a sequence of problems for each order in a_0.

At O(1),

$$\begin{aligned} \frac{\partial u_1}{\partial t} - v_1 &= 0, \\ \frac{\partial v_1}{\partial t} + u_1 &= 0, \\ \frac{\partial \theta_1}{\partial t} - u_1 &= 0, \end{aligned} \tag{3.3a,b,c}$$

with solutions

$$\begin{aligned} u_1 &= A \sin(t - \phi), \\ v_1 &= A \cos(t - \phi), \\ \theta_1 &= -A \cos(t - \phi) = -v_1, \end{aligned} \tag{3.4a,b,c}$$

where the amplitude A and the phase ϕ of the inertial oscillation described by (3.4) are functions of the slow time τ.

Since

$$a = a_0 e^{-m_1(\theta - \theta_0)} \equiv a_0 e^{-m_1 \theta'}, \tag{3.5}$$

the next order problem yields

$$\begin{aligned} \frac{\partial u_2}{\partial t} - v_2 &= -\frac{\partial u_1}{\partial \tau} + u_0(1 - e^{-m_1\theta'}) - u_1 e^{-m_1\theta'} \\ \frac{\partial v_2}{\partial t} - u_2 &= -\frac{\partial v_1}{\partial \tau} + v_0(1 - e^{-m_1\theta'}) - v_1 e^{-m_1\theta'}. \end{aligned} \tag{3.6a,b}$$

Using the fact that u_0 is $O(a_0)$ and hence negligible, it follows that (3.6) may be rewritten:

$$\begin{aligned} \frac{\partial^2 v_2}{\partial t^2} + v_2 &= 2\frac{\partial}{\partial \tau}[A \sin(t - \phi)] + m_1 v_0 A \\ &\times \sin(t - \phi) e^{-m_1\theta_1} + 2A \sin(t - \phi) e^{-m_1\theta_1} \\ &+ m_1 A^2 \cos(t - \phi) \sin(t - \phi) e^{-m_1\theta_1}. \end{aligned} \tag{3.7}$$

There are forcing terms on the right-hand side of (3.7) that have the period of the inertial oscillation shared by the solutions of the homogeneous form of (3.7). Eliminating such resonant terms (which would otherwise invalidate the asymptotic expansion for the pertubation) yields an evolution equation for A.

Consider the case of incipient instability of the steady solutions so that A is small. In that case, ϕ can be shown

to be constant and A satisfies

$$\frac{\partial A}{\partial \tau} + \left(1 - \frac{m_1}{2}\right)A = 0. \tag{3.8}$$

Amplitude growth on the long time scale is therefore predicted only if

$$m_1 = -\frac{1}{a}\frac{da}{d\theta} > 2. \tag{3.9}$$

Figure 4 shows $v(t)$ as calculated from (2.2) for m_1 = 1.5, 1.9, 2.0, 2.1, 2.2, and 2.5. For $m_1 < 2$, the amplitude of the inertial oscillation decreases with time. At these values, the solution will eventually decay to the steady solution. For $m_1 = 2$, the oscillation maintains itself at its initial amplitude with no perceptible growth or decay. For $m_1 > 2$, the inertial oscillation has an amplitude that grows with time in agreement with the prediction of (3.8). The oscillations are locally

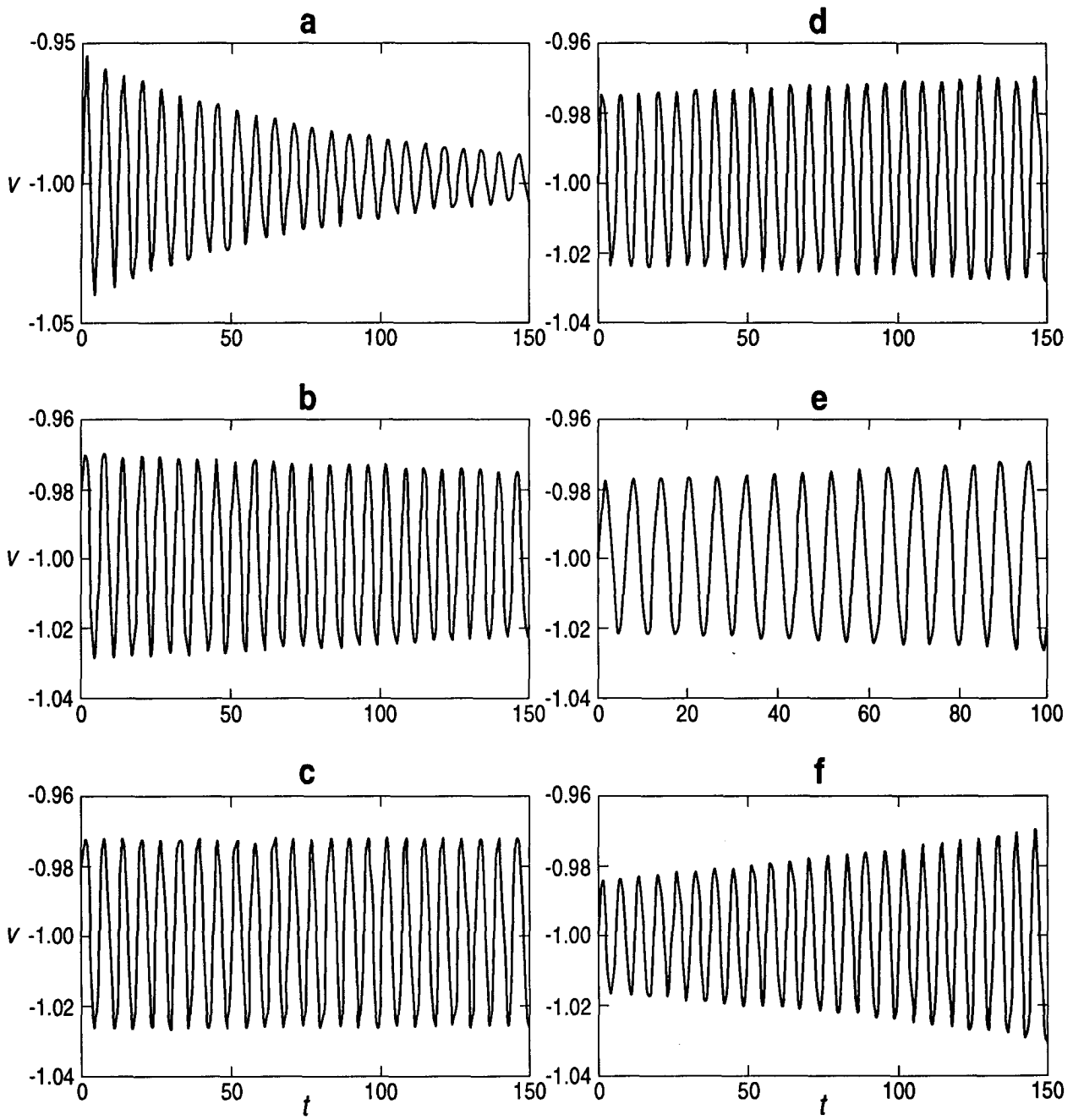

FIG. 4. The evolution of a small disturbance in the case of the "soft" instability $a_m = 0.2$. In (a) $m_1 = 1.5$, (b) $m_1 = 1.9$, (c) $m_1 = 2$, (d) (2.1), (e) (2.2), and (f) (2.5). The transition to instability occurs clearly at $m_1 = 2$.

(in time) inertial oscillations. The period is 2π ($2\pi/f$ in dimensional units), and the relation between u and v as shown in the phase plane is exactly what is expected of inertial motion. The growth is clearly due to the temperature dependence of the dissipation parameter as determined by the criterion (3.9).

The oscillation amplitude will continue to grow until its amplitude eventually equilibrates. Figure 5 shows the oscillation out to $t = 500$, that is, for about 80 inertial periods. The amplitude has equilibrated to a value of $A = 0.376$ for $m_1 = 2.2$.

For

$$\Delta = \frac{m_1}{2} - 1 \ll 1, \tag{3.10}$$

expansion of the exponentials on the right-hand side of (3.7) yields the following nonlinear equation for the amplitude A:

$$\frac{\partial A}{\partial \tau} - \Delta A + \frac{m_1^2}{8} A^3 = 0. \tag{3.11}$$

This yields an equilibrated amplitude, A_e, such that

$$A_e = \frac{(8\Delta)^{1/2}}{m_1} \approx (2\Delta)^{1/2}, \tag{3.12}$$

since $m_1 \sim 2$ for small Δ. We find that the prediction of (3.12) is accurate to about 15%. Thus, for $m_1 = 2.2$, for which $\Delta = 0.1$ (and thus $\Delta^{1/2} \sim 0.3$—not terribly small), (3.12) yields A_e of 0.447, while, as shown in Fig. 5, the numerical result is an amplitude equilibration at the smaller value $A = 0.376$.

This analysis of the "soft" instability in which $a(\theta)$ is a smooth function of θ illustrates the possibility of the self-excited oscillations. In the next section, the case closer to our original qualitative discussion is described, in which $a(\theta)$ is given by the abrupt (or "hard") laws (2.6) or (2.7).

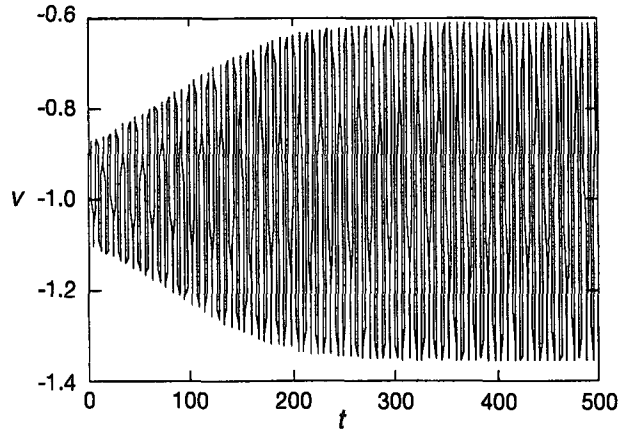

FIG. 5. The eventual equilibration of the amplitude of the soft instability for the case $a_m = 1$, $m_1 = 2.2$.

4. "Hard" instability

The physical process outlined in the Introduction for the sustained inertial oscillations in the presence of steady forcing has the nature of a relaxation oscillation. That is, when the stratification is weak or vanishing, we expect mixing to annihilate the momentum in the baroclinic oscillation. Then, as the mixing itself disappears, the cycle restarts as the layer once again attempts to adjust geostrophically to the large-scale mixing.

The abrupt or "hard" laws of (2.6) or (2.7) partially capture this behavior. However, as formulated, they possess one important deficiency.

Once a solution enters the high-friction parameter region, it will be permanently captured by the steady solution (2.8) and will remain there since the steady solution for $a_0 \gg 1$ will be stable. In the more complex, conceptual model, this steady solution capture is avoided by supposing that a is also a function of shear and vanishes as the shear vanishes. Here we are trying to avoid such a complex and, indeed, arbitrary specification of the mixing coefficient. Clearly, our simple dynamics hardly justifies an elaborate mixing law. Instead, a_h, a_c, and θ_c in (2.6) and (2.7) will be chosen so that the low-stratification steady solution is generally not available to the system. That is, we will choose $a(\theta)$ to look like curve (b) in Fig. 2 rather than curve (a). This places an upper bound on a_c and θ_c. We also choose a critical stratification, θ_c, which is positive but not large enough to provide the low-temperature capture that would be occasioned by the parameters of curve (a) in Fig. 2.

As an example, Fig. 6 shows the sustained oscillation that occurs when $\theta_c = 0.15$, $a_h = 0.01$, and $a_c = 1.5$, and the continuous law (2.7) is used. Each cycle is very nearly a pure inertial cycle with period $2\pi/f$. In Fig. 6a, we show the time history of v. Figures 6b and 6c show θ and v versus u, respectively. The crosses in Fig. 6c show the position of the *virtual* steady solutions (2.8a,b) where a_0 varies with time since θ varies with t over the cycle. Note that the limit cycle in the u, v plane avoids the low-stratification limit of the virtual center at $a = a_c$.

To emphasize the point that the persistence of the oscillation is due entirely to the presence of the *high* dissipation experienced by the fluid when $\theta < \theta_c$, we present in Fig. 7 the result of the same calculation when $a_c = a_h = 0.01$, so that the dissipation is uniform and small. The inertial oscillations are clearly spiraling into the steady solution at $v \approx -1$, $u \approx 0$. The inference we draw is that the cycle is sustained by the continuing suppression of the velocity by dissipation, once per cycle, which allows the imposed pressure gradient to knock the system loose for another attempt at geostrophic adjustment. This process somewhat reminds us of the elegant escapement mechanism of a well-constructed grandfather pendulum clock. Our Coriolis

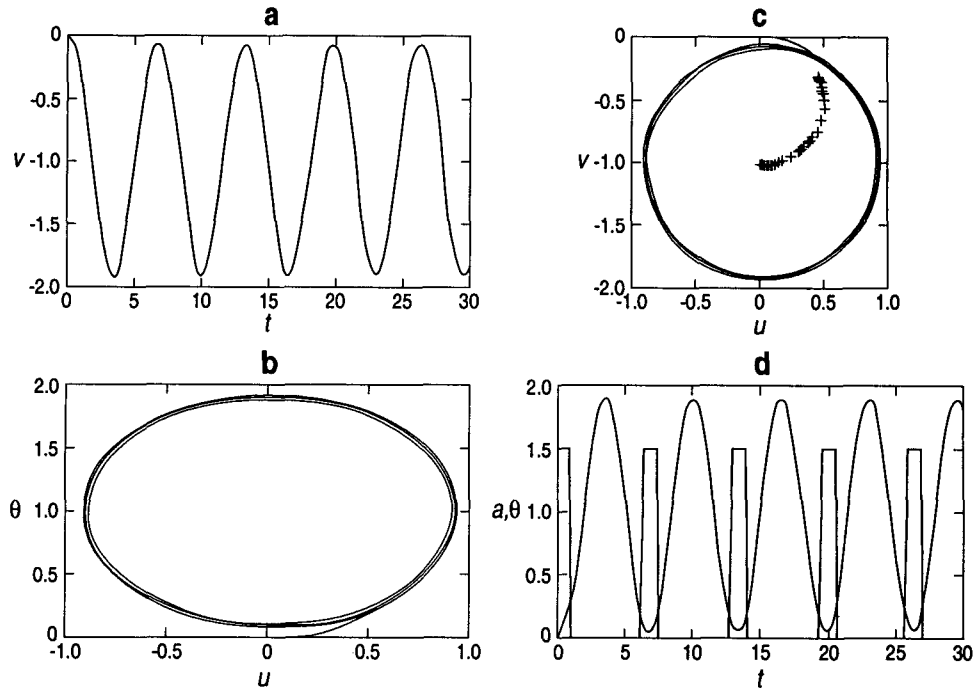

FIG. 6. The limit cycle for the "hard" dissipation law, $a_c = 1.5$, $a_h = 0.01$, $T_c = 1.5$. Panel (a) v versus t, (b) v versus u—the crosses show the positions of the virtual equilibrium solutions during the cycle, (c) θ versus u, and (d) θ and $a(\theta)$ versus t.

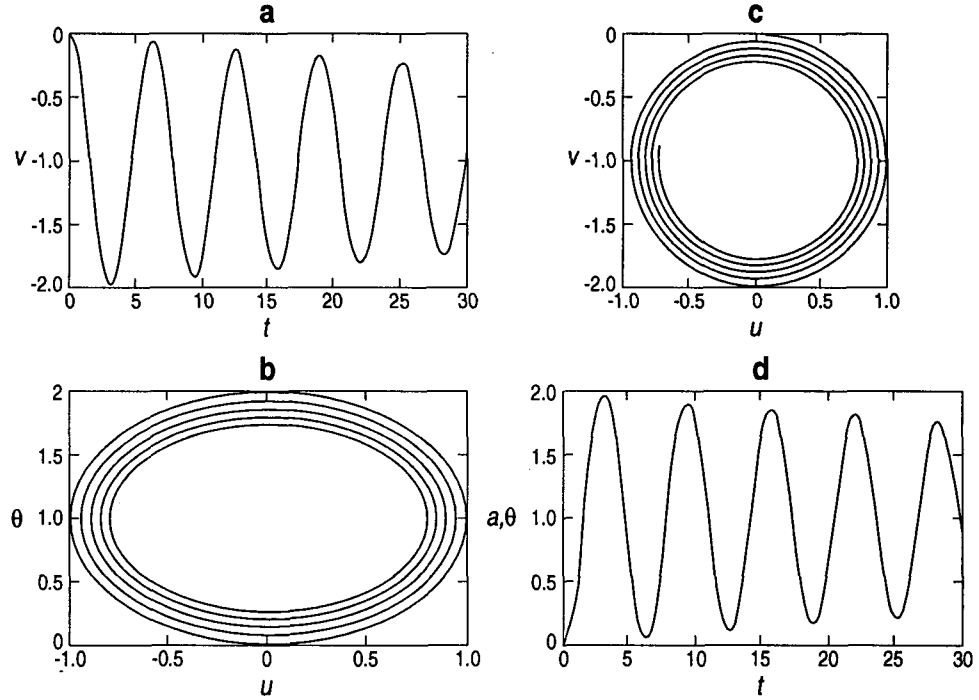

FIG. 7. As in Fig. 6 but for constant *small* dissipation; that is, $a_c = a_h = 0.01$. The solution is spiraling in to capture at the geostrophic steady solution.

escapement mechanism, however, is so particular that a detailed comparison would most likely only further strain the reader's credulity or patience while adding little to a dynamical understanding of the process.

The amplitude of the oscillation may be estimated in the case where the oscillation has the simple form of Fig. 6 as follows.

As Fig. 6d shows, a is essentially zero unless $\theta < \theta_c$ and is constant and equal to a_c in the brief interval when $\theta < \theta_c$. For the oscillation in Fig. 6 we have, very nearly,

$$v_a = u_0 \cos t,$$

$$\theta = 1 - u_0 \cos t,$$

$$u = u_0 \cos t,$$

so that the energy integral over the cycle becomes

$$\bar{a} u_0^2 = \overline{a v_a}. \tag{4.1}$$

However,

$$\bar{a} \approx 2 t_0 a_c,$$

where t_0 is the half-interval of time for which $\theta < \theta_c$, while

$$\overline{a v_a} = u_0 \overline{a \cos t} \approx 2 a_c \sin t_0, \tag{4.2}$$

and where t_0 is determined by the condition

$$u_0 \cos t_0 = 1 - \theta_c. \tag{4.3}$$

It follows that

$$\frac{\sin 2 t_0}{2 t_0} = 1 - \theta_c. \tag{4.4}$$

For the parameters of Fig. 6, this yields $t_0 = 0.475$ and $u_0 = 0.96$, in excellent agreement with the numerical result of Fig. 6.

As θ_c is increased, the curve (b) in Fig. 2 will approach the dashed curve representing the steady solution. Before the curves meet, the self-sustained oscillation changes its structure. Figure 8 shows the oscillation for $\theta_c = 0.33$. For this value of θ_c, there is no low-temperature equilibrium solution, but the distance of curve (b) from the steady solution is small. Now the phase plane of v versus u or θ versus u has a strange, cracked-egg shape with an indentation near the extreme low-temperature limit of the virtual solution in the (v, u) plane. During that portion of each oscillation in which the trajectory in the (u, v) plane approaches the extreme virtual solution (where the eggshell is cracked) both v and u change very slowly. This leads to a significant increase in the period of the oscillation. Whereas the oscillation in Fig. 6 has a period of very nearly $2\pi/f$, the period of the oscillation in Fig. 8 is longer and very nearly $9/f$.

5. Discussion

We have demonstrated a rather curious process whereby a steady, large-scale temperature gradient can

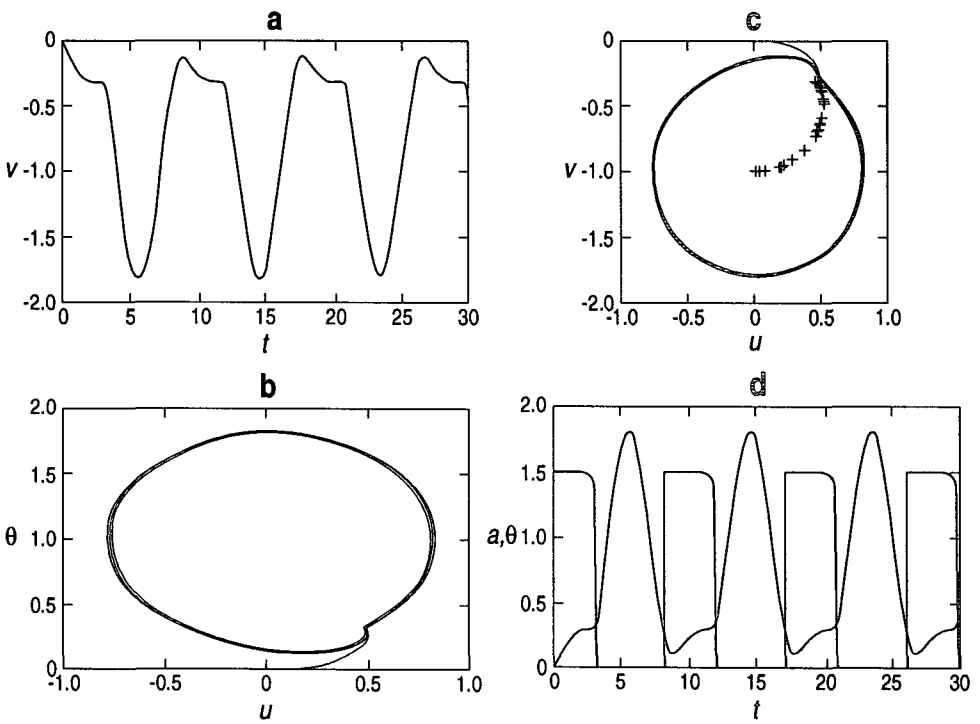

FIG. 8. As in Fig. 6 but for $T_c = 0.33$.

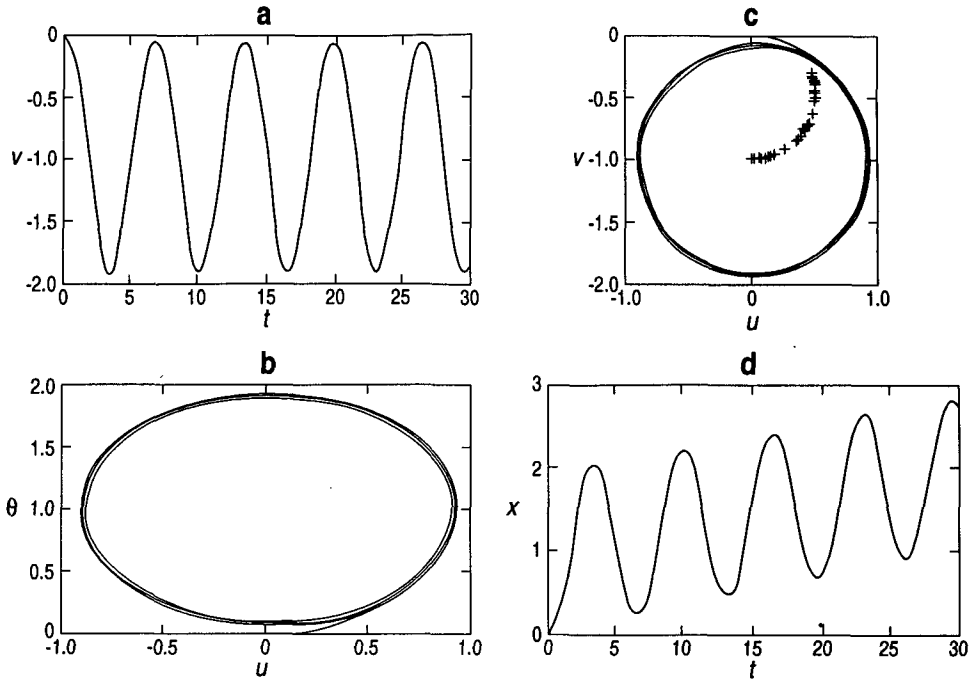

FIG. 9. As in Fig. 6 except that (d) shows the excursion of fluid elements in the x direction.

maintain permanent inertial oscillations in the face of continuous dissipation. At the heart of the process is the system's inability to reach a geostrophic equilibrium due to variations of the dissipation over the cycle of the response. The increase of dissipation with decreasing stratification leads to a perpetual process of disequilibrium, and each attempt to reach adjustment plunges the system into an oscillation about its putative equilibrium.

The energetics of this system is interesting. Close attention to the asymmetry of the v, u phase plane in either Fig. 6 or Fig. 8 shows that it is not symmetric. There is, instead, a net migration of fluid elements down the pressure gradient as shown in Fig. 9d, which delivers sufficient energy to the system to maintain the limit cycles against dissipation.

At this point, we certainly do not present observational evidence to substantiate the relevance of the process in the ocean. We rather think of the dynamics discussed here as primarily illustrative of a robustly simple way in which mixing can pump energy from steady forcing fields into inertial oscillations.

Acknowledgments. J. P. is supported in part by a grant from the National Science Foundation's Division of Atmospheric Sciences. H. S. was supported by National Science Foundation Grant OCE 89-13128.